Computer Generated Microwave Kinoforms

by

Neal C. Gallagher
School of Electrical Engineering
Purdue University
W. Lafayette, IN 47907

and

Donald W. Sweeney
Sandia National Laboratories
Livermore, CA 94550

Abstract

Reflective computer-generated holographic elements are used in a quasi-optical fashion to modify both the phase and polarization of a high-power coherent microwave beam. Theory and design for both one and two component systems are discussed as well as some experimental results.

Introduction

Holographic concepts have been used to design a new type of reflective, microwave optical elements that controls both the phase and polarization of a wavefront. The elements transform the wavefront so that after the beam has propagated a prescribed distance in free space, the microwave field has the desired polarization and intensity distribution. The computer-designed HOlographic Microwave Element, called a HOME, is motivated by and designed using the same concepts as a computer-generated kinoform.[1] Since the microwaves of interest here have a wavelength of a few millimeters to a few centimeters, the microwave elements can be fabricated with *hundredth-wave quality* on a 5-axis computer-controlled milling machine.

The particular application of the microwave elements described here is in electron-cyclotron resonant heating (ECRH) of a plasma for magnetic fusion experiments. Microwave radiation is used to heat the thermal barrier region of the plasma in the mirror confinement systems used at Lawrence Livermore National Laboratory.[2] Microwave energy is obtained from a gyrotron microwave vacuum tube which can produce many kilowatts of average power. Unfortunately, the output of the gyrotron does not have the desired intensity distribution or polarization for proper coupling into the plasma. The microwave elements we describe correct both of these problems.

We describe the basic concepts of a single-element HOME device and document its performance. That element is used on the TMX-U experiment at Lawrence Livermore National Laboratory. The basic concept is reviewed in the next section. In this paper, we also describe a significant generalization of the HOME concepts to include multiple elements. In addition to the previous properties of the HOME reflector, this scheme introduces many new degrees of freedom. For example, the design code can now place multiple HOME elements along an extended optical path.

This generalization was required to allow HOME devices to be used in the proposed MFTF-B machine at Lawrence Livermore. The 10 components designed provide heat-

ing along five beams paths at microwave frequencies of 28, 35, or 56 GHz. Because budget constraints have indefinitely delayed construction of MFTF-B, the HOME elements have been designed but not fabricated.

Single Element System

The coherent microwaves are produced by a gyrotron source whose output has been mode converted to the TE_{01} "doughnut" mode with an average power of 200 kW. Unfortunately, the doughnut mode does not provide ideal energy transfer for heating the plasma; there are two problems. The doughnut shape, with low field strength in the center and high field about the perimeter, is quite different from the desired Gaussian field envelope. In addition, the TE_{01} mode is linearly polarized such that the E-field vector is always tangent to the doughnut; vertical polarization is desired. Figure 1 contains an illustration of the initial gyrotron output wavefront and the desired wavefront at the target plane in the plasma; as can be seen, these are quite different patterns. In order to provide the transformation from the source pattern to the desired pattern, a microwave kinoform has been designed, fabricated, and tested. This kinoform is successful in transforming both the source field distribution and polarization into the desired patterns.

The kinoform is a computer-generated element that modifies only the phase of the incident wavefront. Assumptions that are typically made for the design and utilization of kinoforms include scalar wave theory, Fresnel propagation, vertical (horizontal) polarization, and the thin element approximation.[3] Our previous discussion of the gyrotron's TE_{01} mode polarization leads us to doubt the validity of the scalar theory assumption. In addition, the Fresnel approximation does not apply. It is possible, in a manner, to work around these problems. To aid in this understanding, Fig. 2 may be of help. The wavefront cross section and the size of the kinoform element are such that, when compared to the propagation distances, they do not allow the small angle assumption of the Fresnel approximation. Similarly, obliquity factors cannot be ignored. These assertions are verified by experimental results. In addition, beam polarization does affect propagation. Scalar theory may be accommodated by the independent propagation of the vertical and horizontal components from the gyrotron to the kinoform mirror. In this manner, scalar theory may be applied independently to each linear polarization component. In order to create pure vertical polarization for the entire field at the kinoform, a twist reflector is incorporated into the mirror surface of the kinoform;[4] the operation of the twist reflector is discussed later in the paper.

The result of these limitations is that we need to apply rigorous Rayleigh-Sommerfeld scalar diffraction theory to describe the respective propagation of the two field polarization components. We cannot make a thin element approximation because of the off-axis geometry and large size of the reflector (23 cm $\times$ 35 cm), and the vector theory of EM propagation is required to describe the function of the twist reflector. The relevant question is how do we design the kinoform with these restrictions?

The method we employ to design the kinoform is similar to an iterative algorithm first proposed by Hirsch, Jordan, and Lesem in a patent disclosure.[5] As the method never appeared in the journal literature, it was subsequently reinvented by Gerchberg and Saxton[6] and by Gallagher and Liu.[7,8] A number of signal processing schemes have since evolved from this basic method.[9]

Kinoform design

The design procedure can be described with the help of Fig. 3. By starting with the known mode structure of the waveguide output and an initial guess for the mirror surface, the wavefront is propagated to the kinoform mirror surface. The vertical and horizontal polarization components are propagated independently. At the mirror

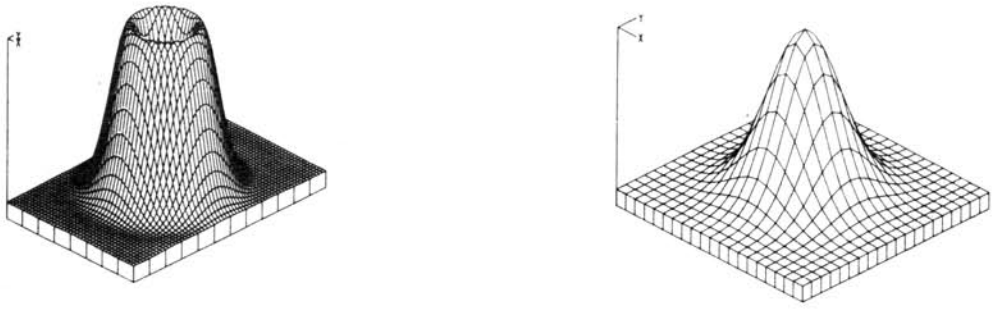

Figure 1. Doughnut shaped wavefront (left) needs to be transformed into a Gaussian shaped wavefront (right).

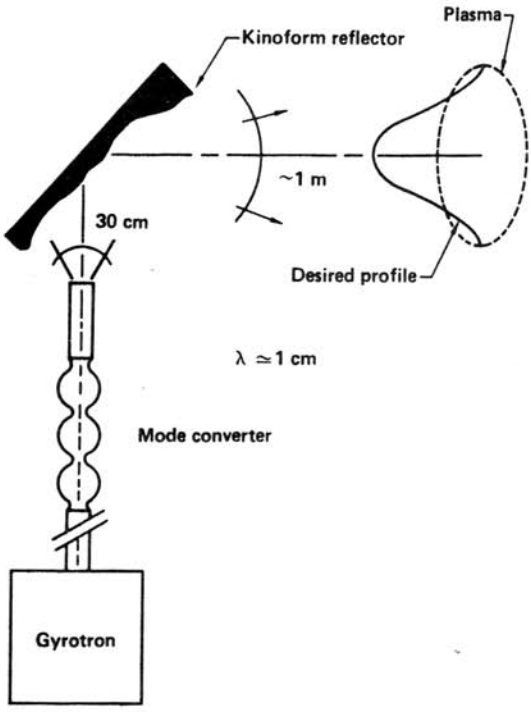

Figure 2. System geometry.

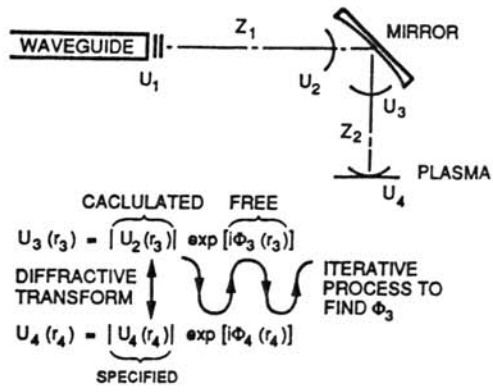

Figure 3.

surface, we assume that the twist reflector shifts the horizontal component into vertical polarization. This new vertical component is combined with the original vertical component so that now the entire field is treated as having pure vertical polarization with an intensity distribution as found in Fig. 4. The propagation is computed using the

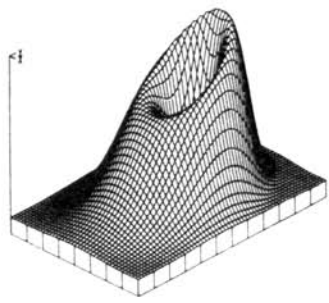

Figure 4. Intensity of wavefront incident on kinoform reflector.

rigorous Rayleigh-Sommerfeld diffraction integral. Fast algorithms, such as the FFT, cannot be employed for this calculation. The iteration now begins. The field is propagated from the mirror surface to the target plane within the plasma, a propagation distance of about one meter. At this plane, the field has some desired intensity distribution; the phase distribution is not important. However, unless we have made an extremely lucky first guess for the mirror surface, the computed field intensity is not the desired field intensity. At this point in the procedure, we impose the desired intensity pattern. We keep the computed phase and then back propagate the field to the mirror surface. The phase distribution of this back propagated wavefront allows us to revise our initial guess for the mirror surface contour. Unfortunately, the field amplitude of this wave will no longer be the correct amplitude; i.e., the amplitude of the wavefront arriving from the source, as shown in Fig. 3; if it were correct amplitude, the design would be complete. We now begin a new iteration. With the correct field amplitude of Fig. 3 and a new phase distribution imposed by the revised mirror, we again propagate to Plane 3. This process is continued until the propagated field intensity in the plasma is sufficiently close to the desired pattern. The procedure converges rapidly to the desired solution; typically, five to ten iterations provide an acceptable design.

The function of the twist reflector cannot be described by use of scalar diffraction theory. It consists of a family of grooves cut into the mirror surface. The duty cycle for these grooves is approximately 50 percent. The period of the groove spacing is less than 1/2 wavelength. The wavelength of our microwaves is about 1 cm. The grooves are cut to a depth of about 1/4 wavelength. A complete analysis for the general curved groove has not been done. However, a rigorous solution for infinitely long strait groove has been completed [10]. It shows, orthogonal polarization will experience a relative phase shift upon reflection from the grooved surface. The following explanation is not intended to provide a rigorous explanation, but only to provide some intuitive visualization. It was with this visualization that lead to the design of the curved grooves actually implemented in the kinoform. Suppose that polarized light strikes such a grooved surface and consider the E-field components that are respectively parallel and orthogonal to the groove orientation. The component parallel to the grooves reflects from the top of the grooved surface. The orthogonal component reflects from the bottom of the grooved surface. It does not "see" the grooves because their period is only $\lambda/4$. Because this component must travel to the bottom of the groove and back out again, a total phase shift of π is introduced on this component as related to the wave which reflects from the groove tops. The result being that the E-field has been "twisted" by the grooved surface. The twisting is such that at each point on the surface, the groove bisects the angle between the incident E-field and the reflected E-field. This is illustrated in Fig. 5. Because the polarization of the field is known at each point on the mirror surface, it is possible to compute the family of grooves that will twist the field at each point on the surface such that the field is everywhere vertically polarized. This groove pattern is shown in Fig. 6. When the grooves are actually milled into the mirror surface, special care must be taken to prevent adjacent grooves from intersecting. In addition, care must be taken to prevent the spacing between grooves from becoming too great; otherwise, the groove structures may act as diffraction gratings, which is very undesirable. For our twist reflectors, the family of possible groove spacings is carefully sorted and grooves are turned "on" or "off" to prevent spacing problems (see Fig. 7).

Kinoform fabrication and testing

A kinoform has been designed for the system illustrated in Fig. 2. The kinoform is designed to produce a Gaussian-like envelope as shown in Fig. 1. After eight iterations in the design procedure, a kinoform surface was computed that yields a nearly gaussian

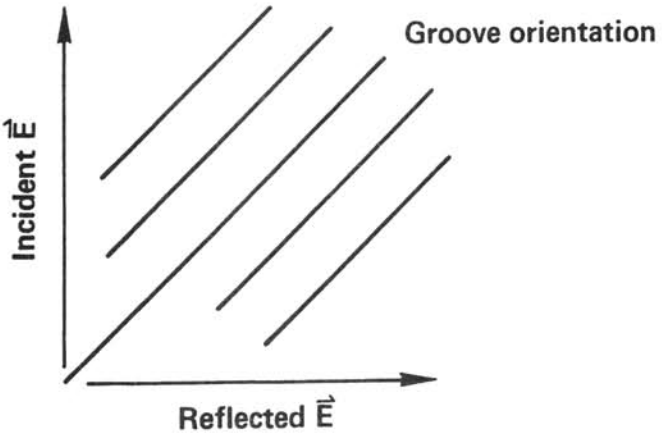

Figure 5. Relationship between incident E-field, twist grooves, and reflected E-field.

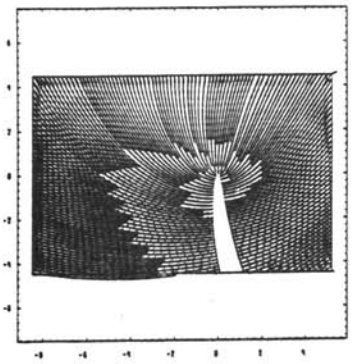

Figure 6. Twist reflector groove pattern.

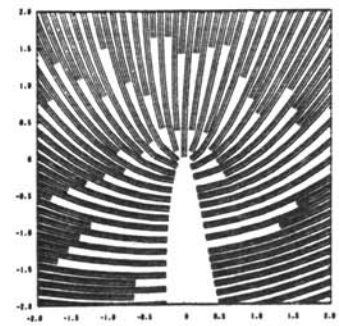

Figure 7. Magnified view of twist groove structure. The diagram shows the centerline and edge lines for each groove. Note how the grooves turn "on" or "off" to keep proper spacing.

plasma plane intensity envelope. This design produces an rms error of about 8 percent between the computed field and the desired field. It should be noted that kinoform phase is unwrapped before the surface profile is computed. This unwrapping avoids surface discontinuities produced with the modulo 2π phase values that are produced by the Rayleigh-Sommerfeld integral calculations.

Kinoform fabrication is accomplished on a Sundstrand computer-controlled five-axis milling machine. The five degrees of freedom for the machining tool are its x, y, and z position, as well as the two direction cosines for the angular orientation of the tool at the surface to be machined. The kinoform is machined in two steps. In the first step, the surface profile computed by the iteration procedure is milled into the surface. For the second step, the grooves of the twist reflector are milled into this mirror surface.

The dimensions of the finished kinoform are approximately 23 cm × 35 cm. Nominally, the total milling time for both steps is about 20 hours; in practice, it has taken somewhat more time.

After fabrication, the kinoform has been tested in a configuration similar to that found in Fig. 2. Figure 8 contains the measured field intensity contour profile for the desired polarization direction as found in the plasma plane. Figure 9 contains a plot of the undesired field polarization in the plasma plane. This test shows that about 95 percent of the field energy has the desired linear polarization. It also illustrates the Gaussian-like intensity profile that the kinoform is designed to produce. With respect to the waveguide source, we note that it has been estimated that gyrotron source output may be contaminated by up to 10 percent with modes other than the TE_{01} mode. This mode contamination will cause degradation in the kinoforms performance. However, if this mode contamination is known, the kinoform can be designed to accommodate these actual wavefronts. Figure 10 shows a photograph of the mirror being made. The tool for cutting the twist grooves can be seen in the corner.

Comments

There are a number of substantial differences between our iteration procedure and those employed in the past.[1,5,6,7,8] First, we are propagating wavefronts over relatively small distances to and from three dimensional surfaces. This is very different from the image plane to Fourier plane type iteration employed in the past. In our procedure, the design surface is actually modified from iteration to iteration; this is different than simply altering the phase of the wavefront in one plane or the other. Because we are actually fabricating an optical element, it is important that phase values used in the surface design by unwrapped from their modulo 2π values. Also, because we are actually designing an element, it is important that the surface be smooth. Consequently, we have found it useful to smooth the kinoform surface with an averaging window at each step of the iteration; this aids in convergence to a smooth design.

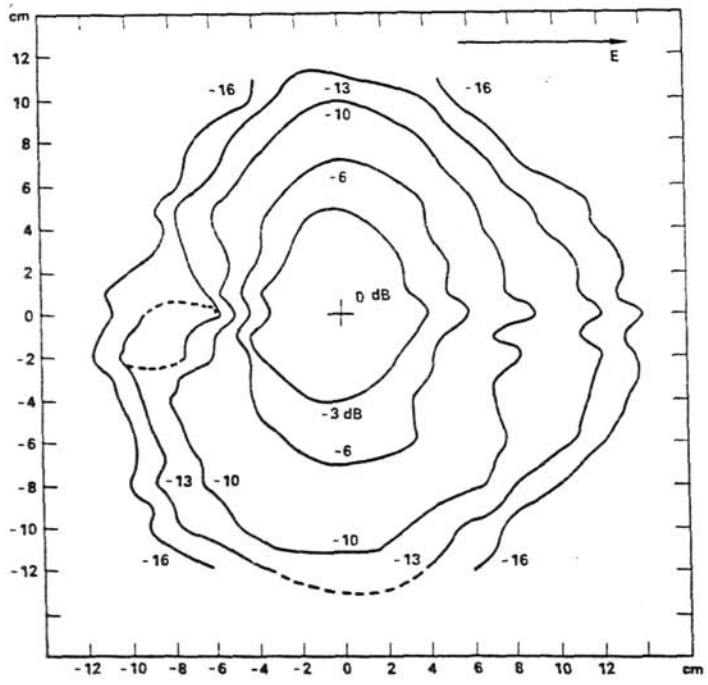

Figure 8. Experimental contour plot of field intensity for the desired polarization component.

As a final remark, we note that by using this method, it may be possible to design elements for infrared or even visible wavelengths. However, questions on sampling requirements and fabrication techniques need to be addressed.

Multi-Element Design Strategy

The basic concepts for multi-element design are depicted in Fig. 11. The figure shows a configuration with two shaped HOME reflectors. Planar mirrors are not shown because they simply fold the optical path in a straightforward manner.

The basic design strategy is to use the first element to correct the polarization of the incident beam so that the final polarization in the plasma will have an electric field aligned with $\hat{E}_3$. Therefore, only Element 1 has an embedded twist polarizer. Element 1 also adds optical focusing power so that the beam-passage diameter can be controlled: this also reduces the size of Element 2. The surface of Element 1 is an off-axis

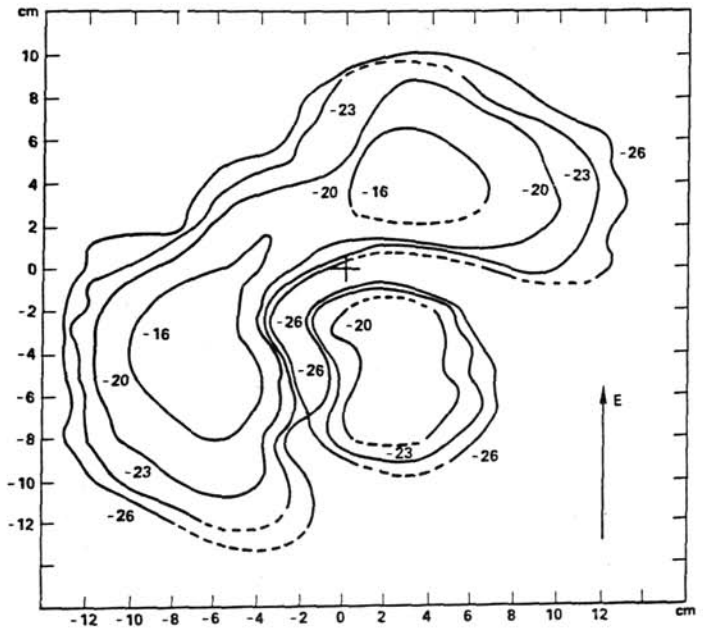

Figure 9. Experimental intensity measurements of undesired polarization component.

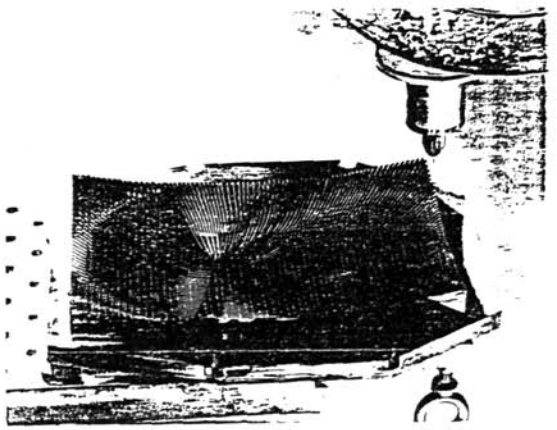

Figure 10. Kinoform being fabricated on five-axis mill.

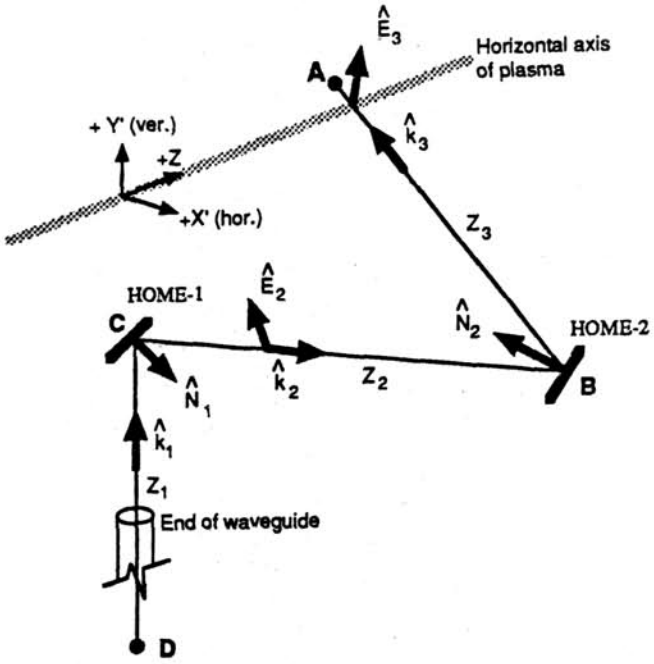

Figure 11. Multi-element Geometry. Individual Elements are not co-planar.

paraboloid; there is no other surface modulation of this element. The groove configuration for the twist reflector is determined by back reflecting $\hat{E}_3$ through Element 2 to produce $\hat{E}_2$. The grooves on the first reflector are designed to be the set of grooves that transform the polarization of the waveguide beam delivery system $\hat{E}_1$ into the desired polarization $\hat{E}_2$.

Element 2 is designed iteratively to produce the desired intensity distribution in the plasma. The iteratively-designed surface modulation of the reflector corrects the phase of the reflected beam so that the diffracted beam will have the proper intensity after free-space propagation to the plasma. The iterative process is essentially the same as described previously. Ideally, the focusing power introduced by Element 1 will provide the primary optical power so that Element 2 needs only to make local corrections to the wavefront phase. Therefore, the optical sag of Element 2 may only be a few wavelengths or less.

Initial design specifications include the spatial coordinates of the plasma, the required intensity and polarization distribution for proper plasma heating, and the overall geometry of the beam path. In some situations, the maximum diameter of the beam passage is also specified. The beam path for MFTF-B is rather convoluted because the beam must pass around other equipment in the system. In general, the distance between elements is several meters and the beam passage is 50 cm in diameter. The design procedure also includes the ability to compensate for multi-mode output from the gyrotron since the mode structure of the microwave gyrotron must be stable for the mirrors to perform properly.

Example of Multi-Element Configuration

A total of five beam paths with two elements each have been designed for MFTF-B. Three beam lines have a frequency of 56 GHz (i.e., 0.534 cm wavelength), one beam path at 35 (GHz, and one beam path at 28 GHz. This section reviews the design of one of the 56 GHz beam paths.

Referring to Fig. 11, the distances Z_1, Z_2, and Z; for this example beam path are 0.8 m, 5.6 m, and 18 ,m, respectively. The included angle between $\hat{k}_1$ and $\hat{k}_2$ is 32 degrees; the included angle between $\hat{k}_2$ and $\hat{k}_3$ is 51 degrees. The wave vectors are not coplanar. At each surface of interest, the electric field must be computed at an appropriate number of sample locations. For this particular example, there were over 15,000 sample locations. This leads to the computational complexity discussed in the next section.

The intensity incident on Element 1 is approximately the same as the far field pattern of the TE_{01} mode. Element 1 is an off-axis paraboloid with a focal length of 0.8 m. The mirror is elliptical with a major axis of 0.5 m and a minor axis of 0.4 m.

Element 2 is also elliptical with axes of 0.6 m and 0.4 m. After several initial computer runs, we determined that an initial surface which was an off-axis paraboloid with a 10 m focal length provided the best results. After seven iterations between Element 2 and the plasma, the phase correction was obtained. The maximum phase correction is slightly over 2π radians. If this phase correction were embedded directly into the surface, one would obtain a true kinoform. Prior to machining, the folded 2π steps are unambiguously removed and the phase correction is converted to a smooth surface relief function. The final surface profile for HOME-2 requires a total sag of 0.5 cm.

For this beam path, proper heating of the plasma requires concentrating the energy with a Gaussian profile with a variance of 15.0 cm the final intensity in the plasma after seven interactions has 85% of the total energy is within the Gaussian envelope. Without the iterative phase correction, only 60% of the energy is within the Gaussian envelope. The 60% figure represents about the best that can be done using classical design procedures.

Discussion

The design procedures described here can become computationally intensive because diffraction theory must be used to propagate between each surface. The reflective element sizes, distances, and wavelengths involved do not allow simplifying Fresnel or Fraunhofer approximations. Each surface must be sampled at an appropriate rate to correctly compute the wavefront. Propagation using the Rayleigh-Sommerfeld diffraction integral imposes a computational burden proportional to the total number of samples on both the input and output surface. If two surfaces have 100 by 100 samples each, then there are 10^8 computational cycles each involving a number of primitive floating point calculations. These calculations must be repeated twice for each iteration between two surfaces.

The design computations described here require about 10 minutes of CPU time on a CRAY-2. In general, several runs are required to obtain a suitable design. The largest number of samples computed on the CRAY-2 were 70×80 on HOME-1 and 80×100 on HOME-2. The output plane of the waveguide and the field in the plasma must also be computed; typically there are over 15,000 sample locations within the system. Since propagation is from one arbitrarily shaped surface to another, there does not appear to be any other computational method that might be able to use fast Fourier methods.

A critical component in the HOME is the twist reflector. During the design and testing of the first components, we realized that the expressions for the complex reflection coefficients must be accurately known to properly incorporate the groove structure in the complex shaped surface.[10] The groove width, depth, and spacing along with the compound angle of incidence all interact to determine the complex reflectance coefficient. Therefore, we have formulated and solved the full EM vector-field describing the twist polarizer. The equations have been solved to date for infinite straight grooves.

Another approximation used previously assumed that the electric field at the exit plane of the waveguide had a field equal to the electric field within the waveguide. A computer calculation now determines the actual free-space field created by the waveguide so that the boundary conditions at the waveguide termination are satisfied.

References

1. Lesem, L. B., P. M. Hirsch, and J. A. Jordan, "The Kinoform: A New Wavefront Reconstruction Device," *IBM J. Res. Develop.* 13, 150 (1969).
2. Stallard, B. W., "Experiment on Hot Electron ECRH in TMX-U," Fifth Topical Conference on Radio Frequency Heating, February 21-23, 1983, Madison, Wisconsin.
3. Goodman, J. W., *Introduction to Fourier Optics,* McGraw-Hill, New York (1968).
4. Hanfling, J. F., G. Jerinic, and L. R. Lewis, "Twist Reflector Design Using E-Type and H-Type Modes," *IEEE Trans. on Antennas and Propagation,* Vol. AP-29, July 1981, pp. 622-628.
5. Hirsch, P. M., J. A. Jordan, and L. B. Lesem, "Method of Making an Object Dependent Diffuser," U.S. Patent No. 3,619,022, November 9, 1971.
6. Gerchberg, R. W. and W. O. Saxton, "A Practical Algorithm for the Determination of Phase from Image and Diffraction Plane Pictures," *Optik* 35, 237 (1972).
7. Gallagher, N. C. and B. Liu, "Method for Computing Kinoforms that Reduces Image Reconstruction error," *Appl. Optics* 12, 2328, October 1973.
8. Liu, B. and N. C. Gallagher, "Convergence of a Spectrum Shaping Algorithm," *Appl. Optics* 13, 2970, November 1974.
9. *Signal Recovery and Synthesis with Incomplete Information and Partial Constraints,* Technical Digest, Optical Society of America, Winter '83, January 12-14, Incline Village.
10. Kok, Y.-L., Gallagher, N. C., "Retative Phases of Electromagnetic Waves Diffracted by a Perfectly Conducting Rectangular-Grooved Grating," J. Opt. Soc. Am. A, 15, pp. 65-73, Jan. 1988.